

# Constrained Flight Test with Gimbal Support System

Taro TSUKAMOTO<sup>\*1</sup>, Masaaki YANAGIHARA<sup>\*1</sup>  
Masakazu SAGISAKA<sup>\*2</sup>

## ABSTRACT

In the ALFLEX project, several constrained flight tests using gimbal support system were conducted before the first automatic landing trial. The purposes of these tests were to confirm the function and performance of the vehicle's control system and to confirm its aerodynamic characteristics. In this report, the stability and performance of the flight control system are studied. In steady or quasi-static flight tests, the vehicle attitude was well stabilized around the trimmed condition. The step command responses for angle of attack, side slip angle, and roll angle were consistent with simulation results.

## 1. Introduction

In the Automatic Landing Flight Experiment (ALFLEX), a gimbal support system is used for the constrained flight before release. In this method, as shown in Fig.1, the vehicle is supported by a cable attached at its center of gravity, so that it can rotate freely around its center of gravity. The merits of this method are,

- (1) A smooth transfer to free flight is expected because there is no restriction of the attitude before release and the control is started before release.
- (2) The function and the characteristics of the control system can be confirmed in the constrained flight condition.
- (3) It is possible to confirm the aerodynamic characteristics of the vehicle in the constrained flight condition.

In the hanging flight test, which was conducted before the automatic landing experiments, it was confirmed by the combined or constrained flights that the onboard systems and the ground facilities worked satisfactorily in flight conditions. In most of these

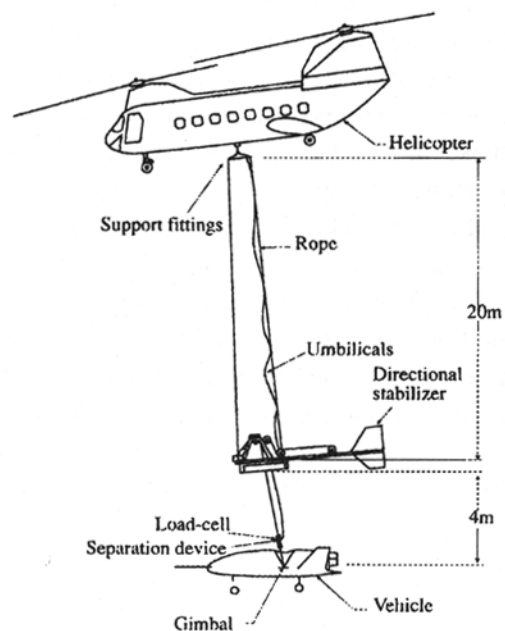


Fig.1 Constrained Flight

tests, constrained flights were implemented to accumulate data for (2) and (3), above. The results showed that the aerodynamic characteristics agree with those predicted from the wind tunnel tests.<sup>1)</sup> Here, comparison with the simulation confirmed that the control system possessed the expected characteristics.

<sup>\*1</sup> National Aerospace Laboratory

<sup>\*2</sup> National Space Development Agency of Japan

## 2. How to evaluate the control system by constrained flight

We consider the problem of how to evaluate a control system for free flight by constrained flight test.

First, the control system for the constrained flight is almost the same as that for free flight. The control block diagram of ALFLEX is shown in Fig. 2. At the time of constrained flight, there is no pitch rate command ( $q_c$ ) from the guidance law; the  $q_c$  command is generated from angle of attack,  $\alpha$ . However, the control law for constrained flight and free flight are one and the same. Therefore, it was expected that the function and characteristics of the free flight control system could be directly confirmed by a constrained flight.

Of course, in constrained flight, the motion characteristics of the vehicle does not agree perfectly with that in free flight, because in the former, the vehicle is constrained by the cable and the flight conditions such as airspeed, attitude and so on differ from those in the latter. However, if the control system shows the performance predicted by its mathematical model in constrained flight, it is expected that it will also show the performance predicted by the same model in free flight.

In addition, in the case of ALFLEX, stability margins for constrained flight are tighter than those for free flight. Table 1 shows the stability margin of

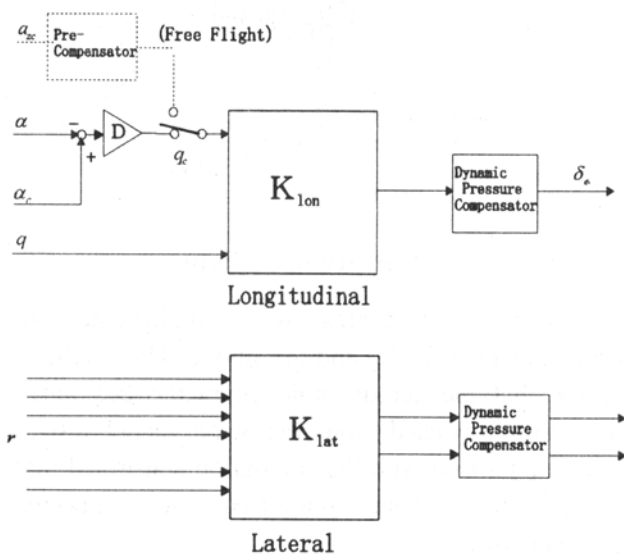


Fig.2 Constrained Flight Control System

Table 1. Gain margins and phase margins

	$\delta e$ - loop	$\delta a$ - loop	$\delta r$ - loop
Constrained 70kt	7.5dB 35.3deg	5.9dB 21.3deg	7.3dB 33.6deg
Constrained 90kt	7.6dB 36.8deg	6.1dB 23.0deg	7.3dB 34.7deg
Release	13.1dB 50.0deg	10.2dB 31.3deg	11.4dB 54.8deg
Diving	13.2dB 51.6deg	10.4dB 33.4deg	11.5dB 57.1deg
Glide slope	14.2dB 54.1deg	11.9dB 49.2deg	11.3 dB 70.7deg
Pre-flare	13.5dB 54.9deg	11.7dB 58.4deg	11.8dB 51.3deg
Landing	13.4dB 53.4deg	11.6dB 56.7deg	12.0dB 49.9deg

each control loop in each flight phase in constrained flight and free flight. It is found that both phase margins and gain margins are most severe in constrained flight. Therefore, if the constrained flight is safely implemented, it is possible to say that the free flight can be more safely implemented from the viewpoint of stability margin.

## 3. Evaluation of stability

### 3.1 Stability in steady flight

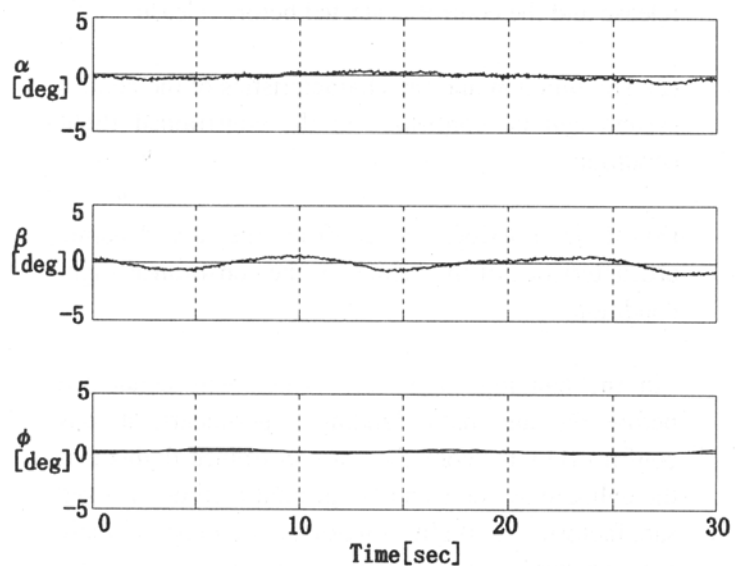


Fig. 3 A Steady 5DOF Constrained Flight (C004)

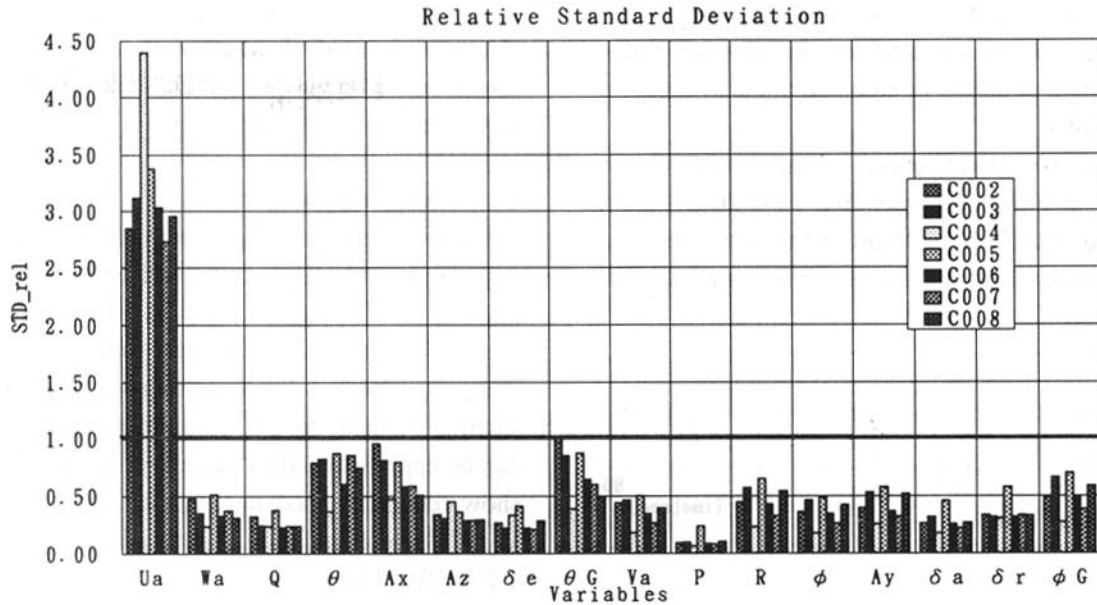


Fig.4 Fluctuations of State Variables in Steady Constrained Flight

Figure 3 shows an example of flight test time history of steady constrained flight. The attitude of the vehicle is stabilized satisfactorily. Figure 4 compares variations of the states in hanging flight tests, where steady constrained flights are realized, with that of simulated flights. The vertical axis is the standard deviation of the states in the flight tests divided by estimated standard deviation by simulation.

The simulation used for the comparison is under maximum design gust condition. The gusts blowing at the vehicle's height in the experiments were not measured. However, considering the pilot's comment that the air was comparatively stable, it must be milder than the maximum gust of the design condition. Therefore, the variation of each state variable should be smaller than that of the simulation.

As for the lateral states, in this plot, the variation of all states are small enough in comparison with the simulation. This shows that the lateral attitude was stabilized satisfactorily.

However, some of longitudinal variables such as airspeed  $U_a$ , gimbal-pitch angle  $\theta_{GBL}$  show larger variation than the simulation. When the variation of  $\theta_{GBL}$  was large, oscillation with a period of about 2-second was found to be dominant (Fig. 5). This is the pendulum mode, which may be excited by the motion of the mother helicopter.

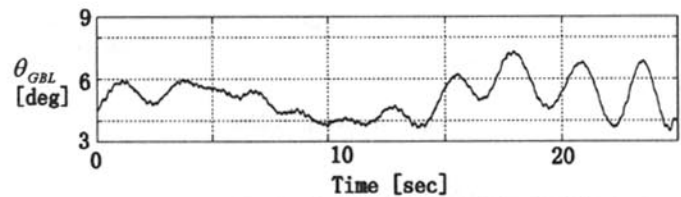


Fig.5 Gimbal Pitch Angle (C005)

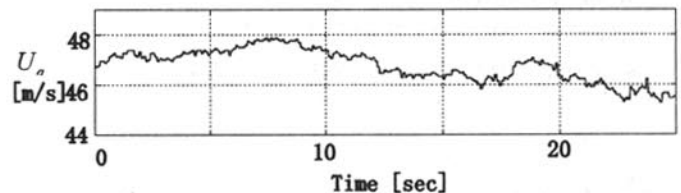


Fig.6 Air Speed in X-direction (C005)

As for  $U_a$ , slower fluctuation is dominant and fluctuation of the mother helicopter speed was directly observed (Fig. 6).

However, these findings are not essential from the viewpoint of comparison of stability between flight test and simulation, because the motion of the mother helicopter, which is exciting these oscillations, is not modeled in the simulation.

### 3.2 Stability in sweep test

Here, the stability in quasi-static flight test named  $\alpha$ ,  $\beta$  sweep is studied. These are the tests in which

the angle of attack or the side-slip angle are continuously varied to confirm the characteristics when the angle of attack or side-slip angle is not zero.

#### (1) $\alpha$ sweep test

Figure 7 shows a representative time history of  $\alpha$  sweep test and the corresponding simulation result. The angle of attack in the flight test was controlled in a stable manner, and the time history resembles that of simulation.

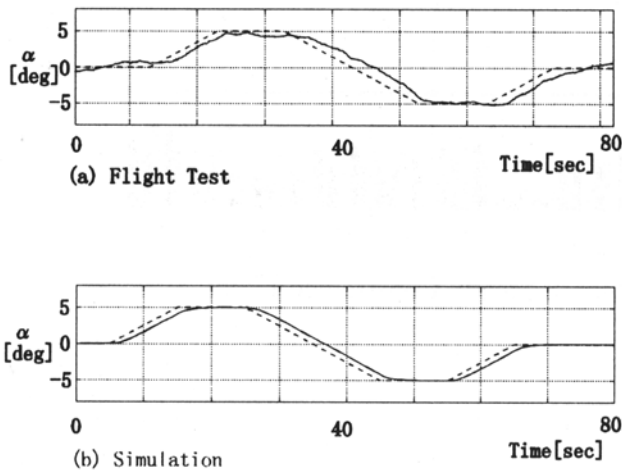


Fig. 7  $\alpha$  Sweep (C004)

#### (2) $\beta$ sweep test

Figure 8 shows a time history of  $\beta$  sweep test and the corresponding simulation result. Because a lateral pendulum mode had been excited before this case, the history of the flight test show a relatively large oscillation but was controlled stably.

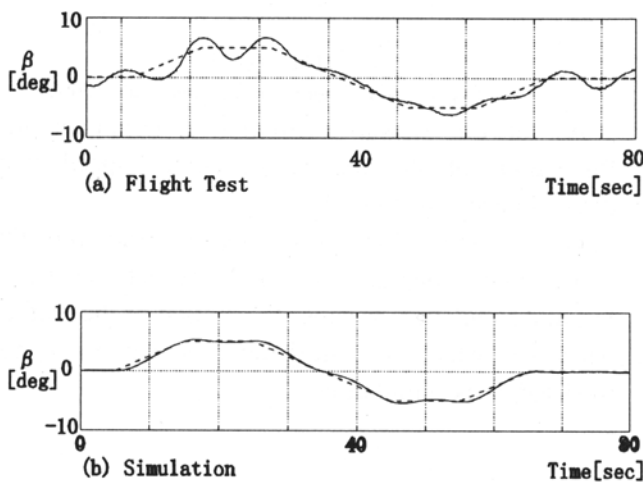


Fig. 8  $\beta$  Sweep (C004)

### 4. Command Response

Next, it is studied whether the response to each command of angle of attack, side-slip angle, roll angle agree with the simulation.

#### 4.1 $\alpha$ step response

Figure 9(a) shows a flight test time history for  $\alpha$ -step command. The command changed from 10 degrees to 0 degrees. (b) is the corresponding simulation time history. Natural frequency  $\omega_n$ , and damping ratio  $\zeta$  are calculated using the least-squares method on the assumption that the system can be approximated by second-order lag. The results show relatively good agreement,  $\omega_n \sim 1.0$  [Hz] and  $\zeta \sim 1.0$  for simulation,  $\omega_n \sim 1.2$  [Hz] and  $\zeta \sim 1.2$  for flight test.

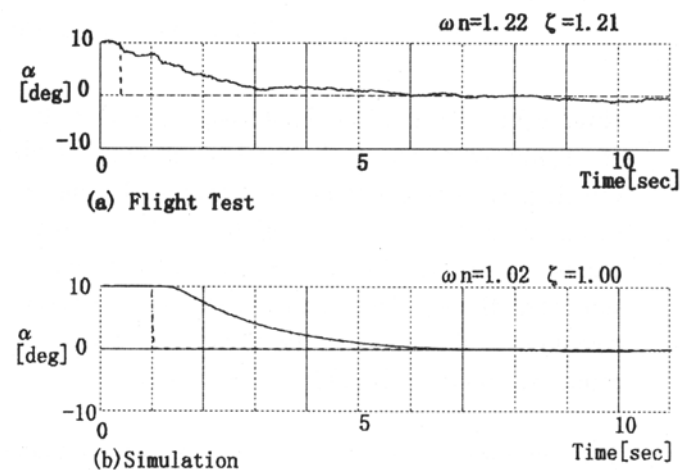


Fig. 9  $\alpha$  Step Response

#### 4.2 $\beta$ step response

A flight test time history for  $\beta$ -step command, from 10 degrees down to 0 degrees is shown in Fig. 10(a); (b) is the corresponding simulation time history. In both of them, the side-slip angle overshoots 0 degrees, then oscillates with a period of nearly 10 seconds, damping slightly. This oscillation is the pendulum-like motion of the vehicle. Again, natural frequency  $\omega_n$ , and damping ratio  $\zeta$  are calculated using the least-squares method on the assumption that the system can be approximated by second-order lag. The results shows relatively good agreement,  $\omega_n \sim 0.6$  [Hz] and  $\zeta \sim 1.2$  for simulation,  $\omega_n \sim 0.5$  [Hz] and  $\zeta \sim 1.2$  for flight test.

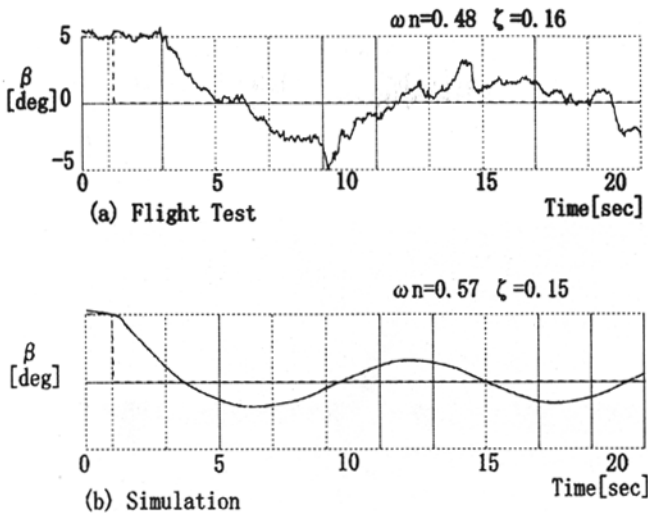


Fig.10  $\beta$  Step Response

#### 4.3 $\phi$ -step response

Figure 11(a) shows a flight test time history for  $\phi$ -step input. It is less disturbed than  $\alpha$  or  $\beta$ , and resembles the simulation result shown in (b).

When calculating  $\omega_n$  and  $\zeta$ , flight test results  $\omega_n \sim 2.6[\text{Hz}]$ ,  $\zeta \sim 0.7$  agrees with the simulation results,  $\omega_n \sim 2.6[\text{Hz}]$ ,  $\zeta \sim 0.7$ .

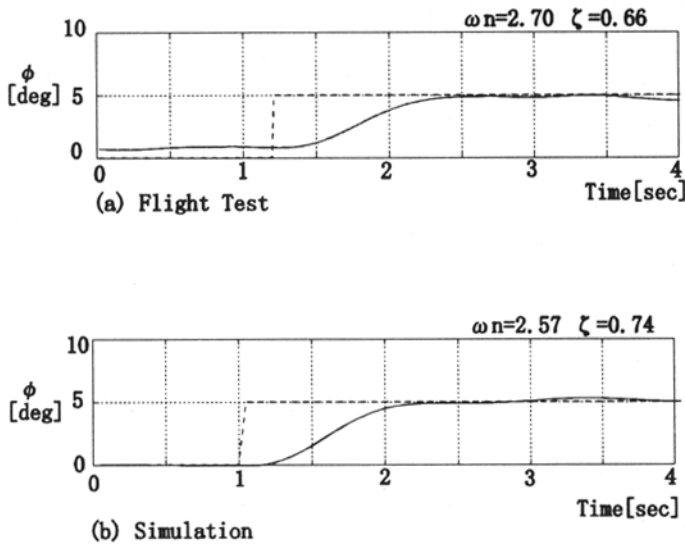


Fig.11  $\phi$  Step Response

#### 5. conclusion

Control system evaluation by constrained flight test was described. It was shown using constrained flight data that the performance of the actual vehicle control system was as expected from the simulation

analysis. Constrained flight tests are an effective method of evaluating a control system.

#### References

- 1) M.Yanagihara, et al, 'Estimating Aerodynamic Characteristics of ALFLEX Vehicle using Flight Test Data', ALFLEX/HOPE symposium, 1996

